Transport analysis of impurities injected by laser blow-off in ECRH and NBI heated plasmas of TJ-II

B. Zurro[1], J. L. Velasco[1], E.M. Hollmann[2], A. Baciero[1], M.A. Ochando[1], R. Dux[3], K.J. McCarthy[1], F. Medina[1], I. Pastor[1], R.J. Hajjar[2], J.M. García-Regaña[3], D. López-Bruna[1], A. V. Melnikov [4,5], L.G. Eliseev[4], HIBP Team[1,4,6] and TJ-II team[1]

[1]*Laboratorio Nacional de Fusión, CIEMAT, Madrid, Spain*

[2]*University of California-San Diego, La Jolla, CA, USA*

[3]*Max Plank Institute for Plasma Physics, Garching, Germany*

[4]*National Research Centre `Kurchatov Institute', 12382, Moscow, Russia*

[5] *National Research Nuclear University MEPhI, 115409, Moscow, Russia*

[6] *Institute of Plasma Physics, NSC KhIPT, 61108, Kharkov, Ukraine*

INTRODUCTION. In previous works in TJ-II, laser blow-off injection (LBI) of BC, LiF, BN and W was used to study impurity confinement in electron cyclotron resonance (ECR) heated plasmas [1, 2]. Herein, the transport analysis of BN impurities injected by LBI into low-density ECR heated plasmas and into higher-density plasmas created during the neutral beam injection (NBI) heating phase of the TJ-II stellarator is studied. These regimes represent two general stellarator regimes: electron-root and ion-root plasmas, respectively. In order to compare these situations, a transport analysis of representative discharges is performed using the impurity transport code STRAHL, from which experimental impurity fluxes are obtained by matching the code results with the temporal behavior of reconstructed local global radiation from bolometer arrays. When compared with neoclassical calculations, poor agreement is found for the low-density plasma while better agreement is found for the latter case. In the higher-density plasma, which is closer to the operational regimes relevant for the stellarator reactor program, impurity accumulation is predicted and observed.

EXPERIMENTAL. The experiment herein reported was performed in the TJ-II a four-period, low magnetic shear stellarator with major and average minor radii of 1.5 m and ≤ 0.22 m, respectively [3]. During the NBI heating phase, higher electron densities are achieved, and in contrast to the ECR heated phase, the density profiles (line-average, $n_e \leq 6x10^{19}$ m^{-3}) are rather peaked whilst the electron temperature profiles are flat with core values in the range 0.3 to 0.35 keV. In addition, the majority ion temperature radial profile is flat with a core value of

around 80-100 eV in ECRH and 120 eV in NBI discharges.

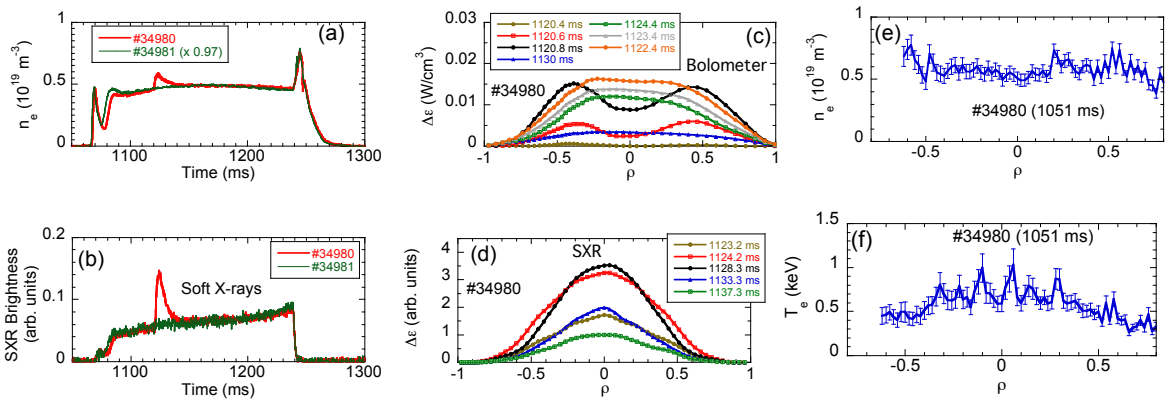

Fig. 1. Traces and profiles of interest for the ECRH shots 34980 with BN injection and reference 34981: (a) line average electron density; (b) soft X-ray (fast photodiode with an 8 μm Be filter), close to the injection port; (c) and (d) incremental emissivity profile evolution during the injection as seen by the bolometer and soft X-ray arrays; (e) and (f) electron density and temperature profiles.

In figure 1 the time evolution of selected signals of interest for two ECRH shots, #34980 with BN injection and the non-perturbed #34981, is shown. In boxes a) and b) the brief duration of the perturbation in line-averaged electron density and in the signal from a fast photodiode with an 8 μm thick Be filter (soft X-ray monitor) positioned close to the injection port, can be observed. In figures 1(c) and 1(d) the time evolution of the incremental emissivity due to the impurity injection, from bolometer and soft X-ray arrays, are shown [4, 5]. Finally, the n_e and T_e profiles are depicted in figures 1(e) and 1(f), respectively.

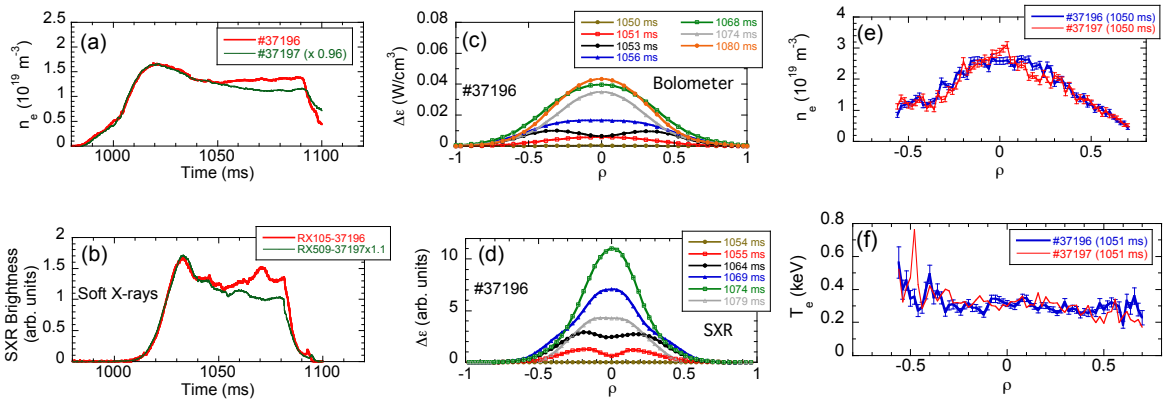

Fig. 2. Similar traces and profiles to those of figure 1, but for the NBI discharges #37196 and #37197 (reference).

Figures 2(a) to 2(f) show information equivalent to figure 1 for two NBI heated discharges: #37196 with BN injection and #37197 without perturbation. As in the previous case, impurity injection strongly affects the monitor signals. However, unlike the ECR heated case, the time evolution of radiation signals shows that the perturbation produced by the impurity injection persists for the remainder discharge duration. This would indicate that the plasma does not expel the injected ions, with the exception of the abrupt expulsion that takes

place at about 1074 ms, simultaneously with a strong MHD event. The effect of BN injection on the line-averaged electron density, depicted in figure 2(a), shows that electrons delivered by the BN tend to remain in the plasma and that the density increases with time, partly because long impurity confinement times allow higher ionization stages to be reached.

Since the radial electric field is one of the key factors in impurity transport, in figure 3 we show the radial profiles of plasma potential, as determined with a 200 keV Cs^+ beam, before BN injection for the two studied discharges [6].

IMPURITY TRANSPORT RESULTS AND DISCUSSION. In order to estimate the experimental impurity fluxes we have proceeded to match, using the impurity transport code STRAHL [7], the temporal behavior of reconstructed global radiation signals measured by a bolometer array, with a similar, but improved, method previously reported [8]. The impurity radial flux is parameterized by two radially-dependent coefficients: a diffusive coefficient D and a pinch V. In order to facilitate the simulation, results of neoclassical calculations [9] are used as initial guesses for D and V. In a first step the iteration method consists in scaling by a factor the theoretical D and V profiles given by the neoclassical theory. The simulation involves an iterative process with the possibility of modifying the transport coefficients as well as several experimentally unknown parameters in the code, *e.g.* impurity radial deposition, transport coefficients profiles, etc., in order to achieve a good match between experimental data and simulation results.

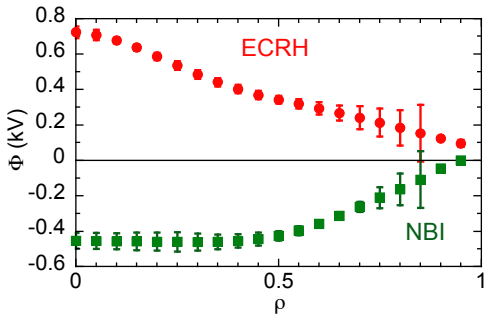

Fig. 3. Plasma potential profiles for the two selected discharges chosen for the transport analysis.

The transport analysis results of the ECRH discharge #34980 and NBI shot #37196, where BN was injected by LBI, are depicted in figure 4. In figures 4(a), 4(b) and 4(c), it is presented the comparison between the experimental D&V coefficients and the radial impurity flux determined by the STRAHL code and the results of neoclassical calculation for the ECR heated case. Similar results for the NBI heated shot are shown in plots 4(d), 4(e) and 4(f) of the same figure 4. The discrepancy in two orders of magnitude in the diffusion coefficient for the low density ECR heated discharge must be highlighted. However, a good agreement is found for the NBI discharge at middle radius but differences about two orders of magnitude are seen at the core and about a factor 10 at the periphery. The agreement is better in the case of pinch coefficients for both discharges.

The splitting between D and V coefficients in the experimental flux may be non-unique; in particular, for short discharges in which the impurity density profile does not reach

a stationary status, the calculation of D may become inaccurate. With this in mind, we also compare the total radial fluxes: in the low-density case, we observe qualitative agreement, although the absolute value is underestimated in the calculations, especially at outer positions (although it could be that the experimental value is overestimated, e.g. due to the effect of non-maxwellianity of the electron distribution function in the ionization/recombination rate coefficients). In the NBI case, prediction and measurement are probably in agreement within the available precision up to r/a=0.6. At outer positions, a radially-localized enhanced diffusion, yet to be understood, is required for explaining the experimental radiation signals.

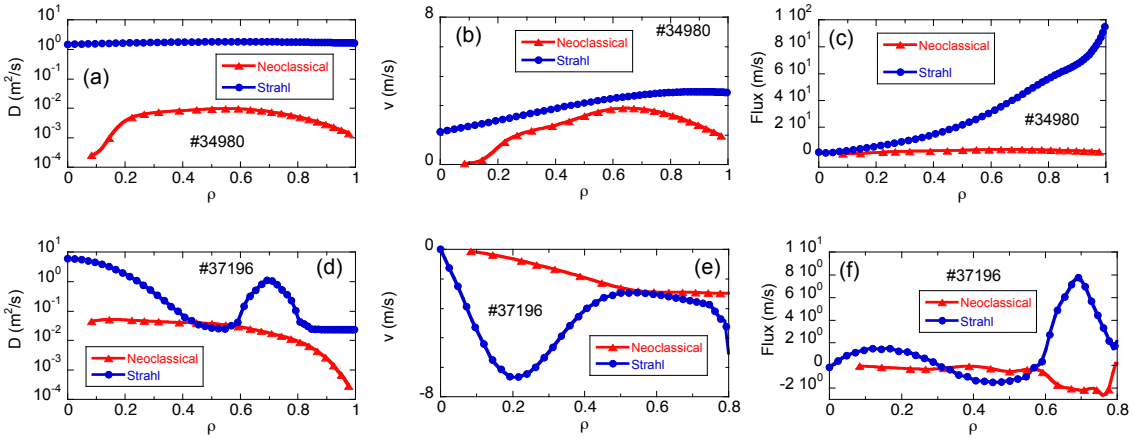

Fig. 4. Comparison of transport results deduced from experimental data, using the STRAHL code and calculated with neoclassical theory: (a) D's for ECRH discharge #34980; (b) V's for the same discharge; (c) Fluxes for #34980; (d) D's for NBI discharge #37196; (e) V's for NBI discharge #37196 and (f) Fluxes for #37196.

Acknowledgements. This work was partially funded by the Spanish "Ministerio de Economía y Competitividad" under Grants No. ENE2014-56517-R and ENE2012-30832, and by the US Department of Energy under DE-FG02-07ER54917. This work has been carried out within the framework of the EUROfusion Consortium and has received funding from the Euratom research and training programme 2014-2018 under grant agreement No 633053. Plasma potential measurement has been carried out by RSF project 14-22-00193. The views and opinions expressed herein do not necessarily reflect those of the European Commission.

References

[1] Zurro B, Hollmann E, Baciero A *et al* 2011 *Nucl. Fusion* **51** 062015

[2] Zurro B. *et al* 2014 *Plasma Phys. Control. Fusion* **56** 124007

[3] Sánchez J., Tabarés F., Tafalla D. *et al* 2009 *J. Nucl. Materials* **390** 852

[4] Ochando MA 2006 *Fusion Sci. & Tech.* **50** 31

[5] Medina F. *et al* 1999 *Rev. Sci. Instrum.* **70** (1) 642-644

[6] Melnikov A.V. *et al*., 2007 *Fusion Sci. Technol.* **51** (1) 31-37

[7] Dux R, 2014 STRAHL User Manual

[8] Zurro B, Baciero A *et al* 2004 *Rev. Sci. Instrum.* **75** 104231

[9] Velasco JL *et al* 2011 *Plasma Phys. Control. Fusion* **53** 11 115014